CR-160296

SPACE CONSTRUCTION SYSTEM ANALYSIS

TASK 3 FINAL REPORT

CONSTRUCTION SYSTEM SHUTTLE INTEGRATION

JUNE 1979

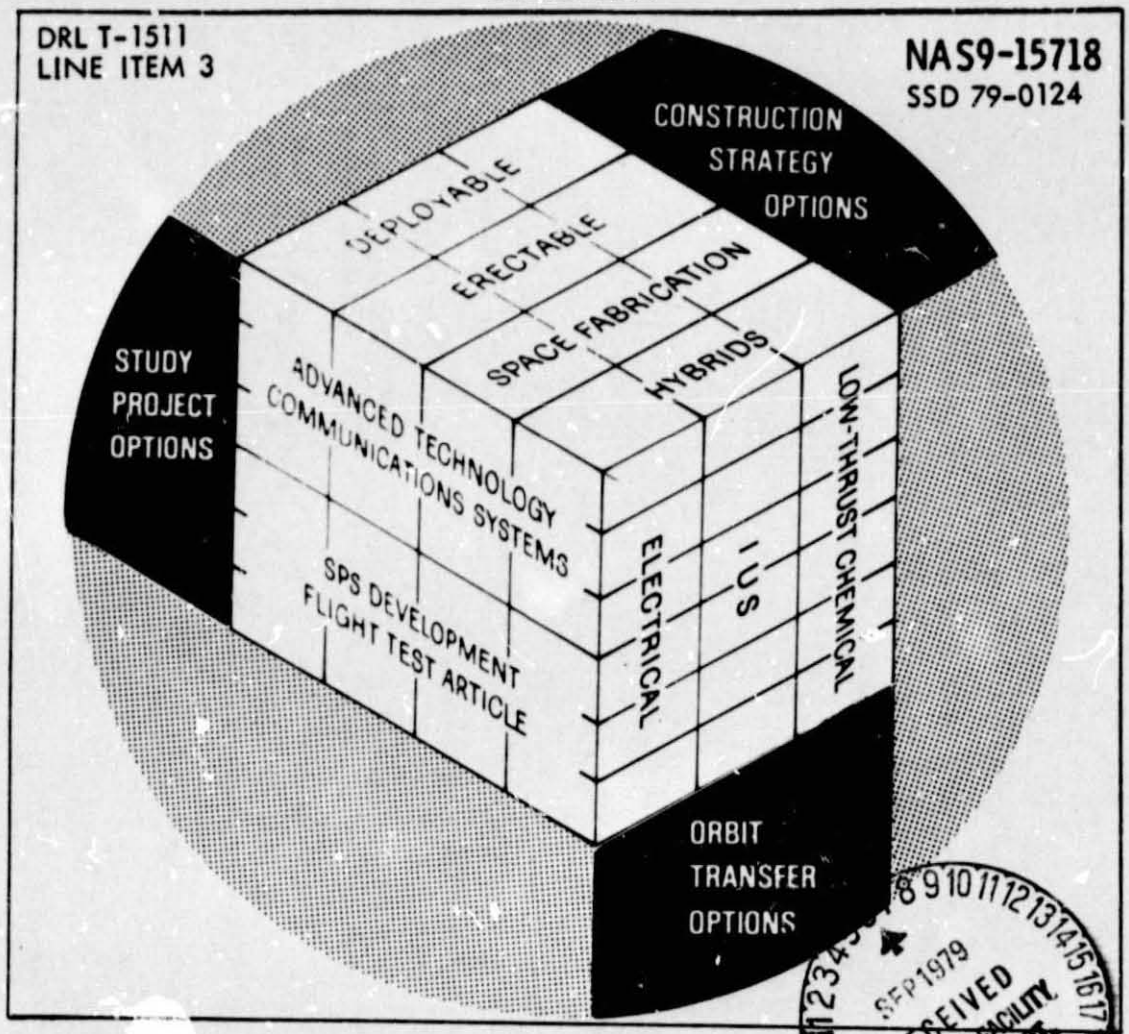

Rockwell International
Satellite Systems Division
Space Systems Group
12214 Lakewood Boulevard
Downey, CA 90241

SSD 79-0124

SPACE CONSTRUCTION SYSTEMS ANALYSIS STUDY

TASK 3 FINAL REPORT

CONSTRUCTION SYSTEM SHUTTLE INTEGRATION

CONTRACT NAS9-15718

DRL T-1511, LINE ITEM 3

JUNE 1979

Approved by:

Ellis Katz
Study Manager

Rockwell International
Space Division

FOREWORD

This report documents the results of Task 3, Construction System Shuttle Integration of the Space Construction System Analysis Study, Contract NAS9-15718. The effort was conducted by the Satellite Systems Division, Space Systems Group of Rockwell International Corporation, for the National Aeronautics and Space Administration (NASA), Johnson Space Center (JSC).

The study was conducted under the direction of Ellis Katz, Study Manager. The following persons made significant contributions to the information contained herein.

R. E. Cook
Dr. E. P. French
J. A. Roebuck
J. Sampson

Major documents resulting from Part I of the contract effort are listed below:

Space Construction System Analysis,
Project Systems and Mission Descriptions,
Task 1 final Report, SSD 79-0077,
April 26, 1979

Space Construction System Analysis, Task 2 Final Report—
System Analysis of Space Construction, SSD 79-0123,
June 1979

Space Construction System Analysis, Task 3 Final Report—
Construction System Shuttle Integration, SSD 79-0124,
June 1979

Space Construction Data Base, SSD 79-0125,
June 1979

Space Construction System Analysis, Special Emphasis
Studies Final Report, SSD 79-0126, June 1979

CONTENTS

ILLUSTRATIONS

TABLES

1.0 INTRODUCTION

Task 1 of the Space Construction System Analysis study was concerned with the design definition of selected system projects; the results of the task are reported in Rockwell Report SSD 79-0077. In Task 2, reported in SSD 79-0123, the flight system projects were analyzed to determine the potential methods for in-space construction of the hardware elements comprising these systems. One of the basic assumptions of Task 2 was that all space construction operations would be conducted from the Shuttle orbiter.

Task 3, the subject of this report, considered the implications and impacts devolving upon the orbiter by its utilization as a space construction facility for the selected flight system projects.

The information presented in this report should be regarded as preliminary and subject to change and expansion as dictated by the end-to-end construction analysis to be performed during Part II of this study.

This report is organized into sections which treat each of the orbiter subsystems and operations for which some measure of construction impact is projected.

2.0 SUBSYSTEM INTERFACES

2.1 ELECTRICAL

There are two major issues regarding the electrical aspects of using the orbiter as a construction base: maximum power and total energy.

The power requirements for construction have been discussed in Section 3.0, Construction Support Services, of Task 2 final report (SSD 79-0123). These are summarized in Table 2.1-1. Since the detailed integrated construction scenario has not been generated, the operations to be performed in parallel have not been identified; thus, the total power requirements are unknown. However, a review of the major power usages from Table 2.1-1 indicates that the individual peak requirements are not likely to be additive. Therefore, there is a good possibility that we can keep within the orbiter capability of 7 kW continuous with 12 kW peaks for 15 minutes every three hours. If the overall construction power profile shows significant times with requirements above 7 kW, four options are available:

1. Reduce parallel power usages—Rescheduling construction activities may be acceptable.

2. Run the dedicated fuel cell at the required power levels—This may cause the fuel cell life to be shortened, but may prove to be more cost effective than other means.

3. Add batteries to handle peak loads and recharge during slack periods—Extra equipment must be mounted in the bay with the resultant payload weight and volume losses.

4. Add new fuel cell—Again, the equipment must be mounted in the bay and the weight and volume penalties accepted.

For all construction operations, the orbiter is expected to be in the standard powered-down mode where the level requirements are 13 kW. In this mode all necessary orbiter systems will be operating.

Even though the 7-kW maximum continuous power provided by the orbiter for construction may be adequate, the 50 kWh of energy definitely will not. Figure 2.1-1 presents the energy requirements as a function of on-orbit construction time. The three baseline orbiter cryo tank sets provide orbiter energy for slightly over seven days, as the orbiter operating at 13 kW continuous requires 312 kWh per day. Therefore, after seven days, the energy to operate the orbiter is chargeable to the construction operation. Thus, there is a sharp increase in energy requirement at this point. As noted in the figure, the energy requirements are based on construction being performed as a two-shift operation, or 16 hours out of every 24-hour period. Three options are available to provide the needed energy; these are discussed below.

Table 2.1-1. Electrical Power Requirements

ITEM	POWER REQ'D (PEAK)	
	SPACE FAB	ERECTABLE
BEAM MACHINE	2 KW	N/A
CONST FIXTURE WELDERS TRANSLATION SWING ARM	2 - 5 KW	2 - 3 KW
RMS	1.8 KW	1.8 KW
MANNED REMOTE WORKSTATION	0.5 KW	0.5 KW
CONST COMMAND AND CONTROL	TBD	TBD
ILLUMINATION	2 - 3 KW	3 KW
CONST CHECKOUT	TBD	TBD

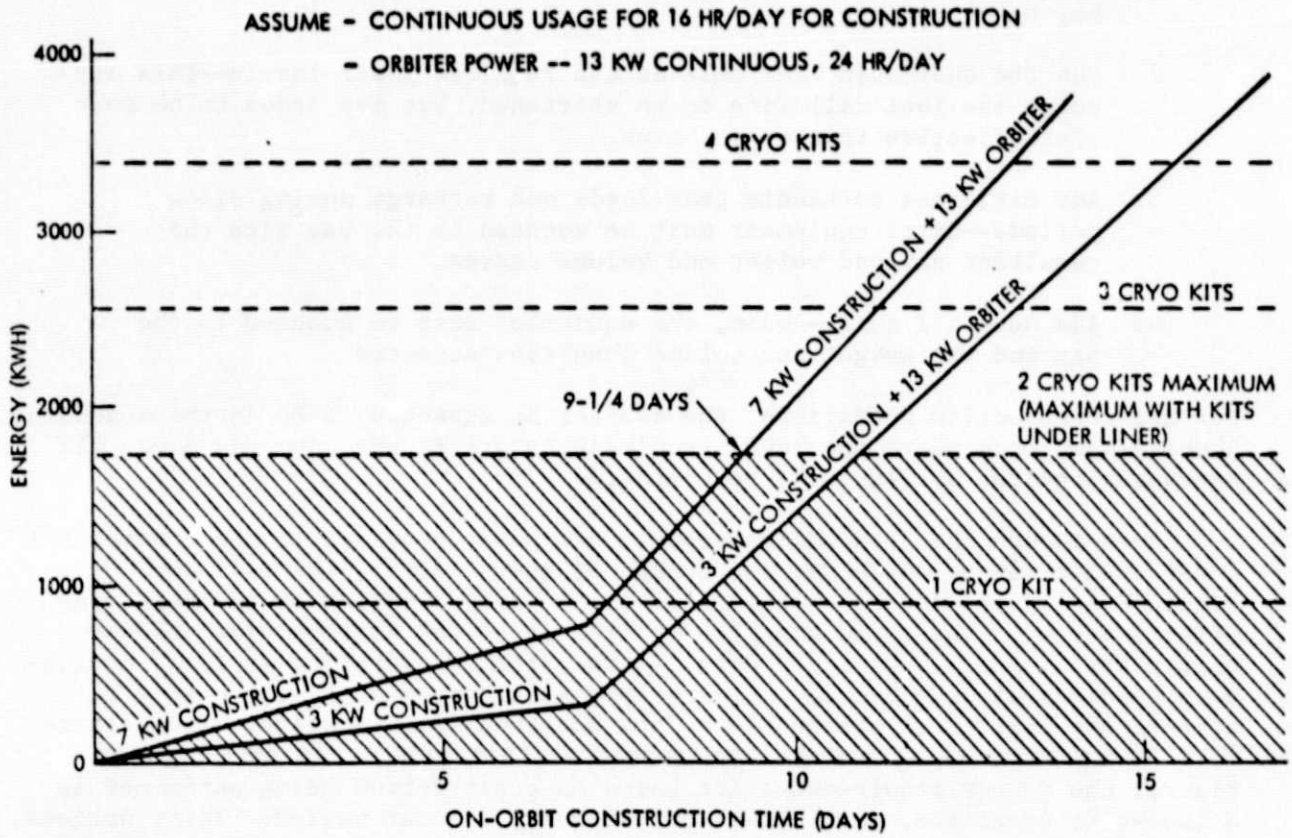

Figure 2.1-1. Power and Energy Availability

- *Option 1. Below-liner cryo kits.* There is currently space for one set (and possibly two) under the liner. Figure 2.1-1 shows that mission times of slightly over nine days can be attained with two tank sets. The fluid and electrical interfaces currently exist for extra cryo tank sets. Thus, no modifications to the orbiter are required.

- *Option 2. Cryo kits in payload bay.* Additional cryo tank sets (1 to 4) can be installed in the bay by the use of a wafer packaging concept as shown in Figure 2.1-2. If the maximum of four sets are used, the mission time can be increased to approximately 13 days (at maximum average power levels). The advantage of installing extra tank sets in the bay with the wafer type of support structure is the shorter installation time. The tanks can be installed in the wafer "off line" (not a part of the payload installation allocation). The installation of the wafer in the bay, including connection of the fluid and electrical interfaces is expected to be considerably less than the time necessary to install and connect individual cryo tanks under the liner. The disadvantage of this option is the use of valuable bay volume (48 inches). Since most construction cargos are volume-limited and not weight-limited, this option may be undesirable.

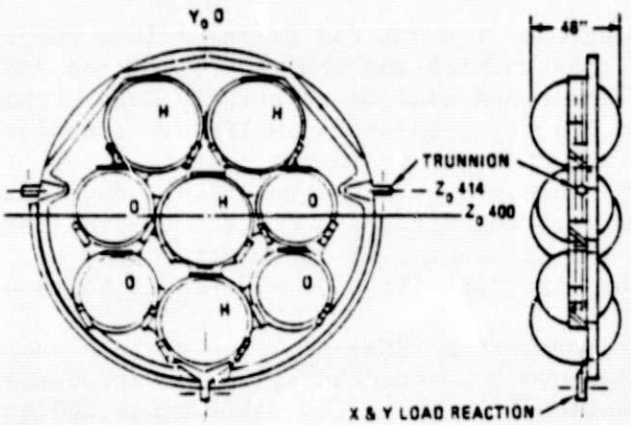

Figure 2.1-2. Alternative Cryo Wafer Kit

- *Option 3. Power extension package (PEP).* PEP would nearly double the maximum mission time from 7 to 14 days without the addition of cryo kits. However, PEP requires a dedicated RMS and probably would require orbiter attitude control during construction to maintain the solar array in the desired orientation.

2.2 AVIONICS

A comparison of space construction requirements has shown all are within the current orbiter avionics capability. Communications between the orbiter, ground, and EVA construction personnel will use the standard UHF, S-band and K-band orbiter equipment with the K-band also used for orbiter to construction fixture rendezvous and docking operations. As with most payloads, space construction will require its special control and display panels at the payload station (PS) of the aft flight deck (AFD). The current thoughts of having the major portion of the construction fixture operations automated and controlled by self-contained hardware and software should result in adequate control and monitoring space and volume capability at the AFD.

2.3 REACTION CONTROL

For normal Shuttle space operations the orbiter reaction control system (RCS) provides the control for rendezvous maneuvers and for attitude control during the mission operations. However, the studies performed on space construction indicate that space construction operations in a free-drift mode are acceptable and, therefore, no attitude control is required when the orbiter is berthed to the construction project. Consequently, the orbiter will command the RCS inhibit mode to prevent RCS firing during construction.

The operation scenario of the RCS for berthing is a function of the geometry of the structure under construction and the control method employed on the structure. In general, the structure will be relatively long, compared to orbiter dimensions, and will be gravity-gradient stabilized. Therefore, the orbiter maneuvers for berthing are unique compared to near-term berthing operations which present-day studies, and man-in-the-loop simulations, have addressed. Secondly, because of the very low attitude stiffness of gravity-gradient control and the large surface areas of the structure, it is required that orbiter operations do not upset or disturb the structure attitude and libration rate.

The remote manipulator system (RMS) promises to be a useful tool for berthing to the platform. Because the structure inertias are comparable to those of the orbiter, the orientation of both bodies will change due to the forces and moments exerted by the RMS. The RCS will be required to provide proper relative orientations without interfering with RMS operation.

The revisit/berthing maneuver, therefore, will require RCS control. This maneuver may require precision RCS control on translation and attitude in order to effect RMS engagement for berthing control. Figure 2.3-1 indicates the region of acceptable initial translation rates and initial rotation rates that will permit safe RMS engagement and, consequently, a successful berthing to the construction project.

RCS issues associated with the berthing operation are (1) possible control system software revisions, and (2) control system capability considering jet inhibit constraints and structure mass properties. The software for orbiter attitude control and jet selection may not be suitable for the unique requirements of berthing large payloads.

Further studies are required to assure RCS control system capability to perform the berthing maneuver required to be within the RMS capture capability.

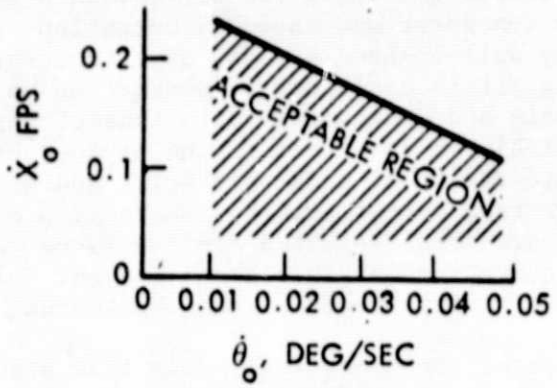

Figure 2.3-1. Closure Requirements

2.4 CREW SUPPORT

None of the individual operations investigated in Task 2 has identified the need for more than three crew members (two EVA and one at the aft flight deck (AFD). Assuming one dedicated orbiter crew member, the basic orbiter capability of 28 man-days of expendables will be exceeded for missions beyond seven days. However, the orbiter has storage capacity for a maximum of 42 man-days (payload is charged with the weight for crew expendables between 28 and 42 man-days and for both weight and volume beyond 42 man-days). The integrated construction analysis may indicate a desirability to perform operations simultaneously, thus increasing the crew size. The addition of the required crew expendables is not expected to create a problem for the construction project, as the individual Shuttle flights are normally not weight- or volume-limited, but dimension-limited. Thus, storage space for relatively small volume of crew expendables packages is expected to be no problem.

The current orbiter capability of two 2-man EVA's for construction will not be adequate if the integrated methods analysis finds the potential of significant EVA operation to be reality. Additional Shuttle-type tanks can be used, each providing nitrogen for approximately 4.5 repressurizations of the airlock (4.5 EVA's). Preliminary indications are that one or more tanks can be added under the payload bay liner. However, modifications to the orbiter will be required for tank mounting and to provide the necessary fluid interfaces for N_2 kits.

2.5 SOFTWARE

It is expected that a significant portion of the automatic operations to be performed by the construction fixtures will be controlled by minicomputers within the fixtures, with only the basic functions controlled through the orbiter computer. Software for basic operations to provide orbiter damage avoidance control for the RMS and RMS/cherry picker will be required.

2.6 LIGHTING

Space construction operations using the orbiter as a base are characterized by requirements for some transport and assembly operations at considerable distance from the relatively well-lighted payload bay. However, to minimize power demands for such lighting, it is desirable to perform as many as possible of the critical, detailed assembly and deployment operations of smaller components, struts, modules, etc., within or very near to the payload bay. This guideline must be tempered by consideration of cargo packaging and use of docking ports which may block off light from certain lamps. Where TV cameras are used to perform or observe remote operations, selected orbiter lamps (as well as others for construction) may require special shields to prevent "blooming" of the images of the lamps when directly viewed by the TV cameras.

A significant portion of the electrical power load discussed in Section 2.1 may be devoted to illumination of construction fixtures, construction equipment, and the project itself. To hold such power and energy demands to a minimum, a variety of approaches have been described and discussed in the Task 2 final report, System Analysis of Space Construction (SSD 79-0123). Figure 2.6-1 illustrates several types of lamps which may be used in a typical integrated construction operation. The key concept for selection and location of such luminaires is to use a small number of lamps to efficiently illuminate only the critical work areas and transport obstacles, and then only when work is actively going on in the vicinity of such areas. Implementation of this approach involves turning off any specialized lamps not specifically needed for a current task by means of switches on the payload control console in the orbiter cabin.

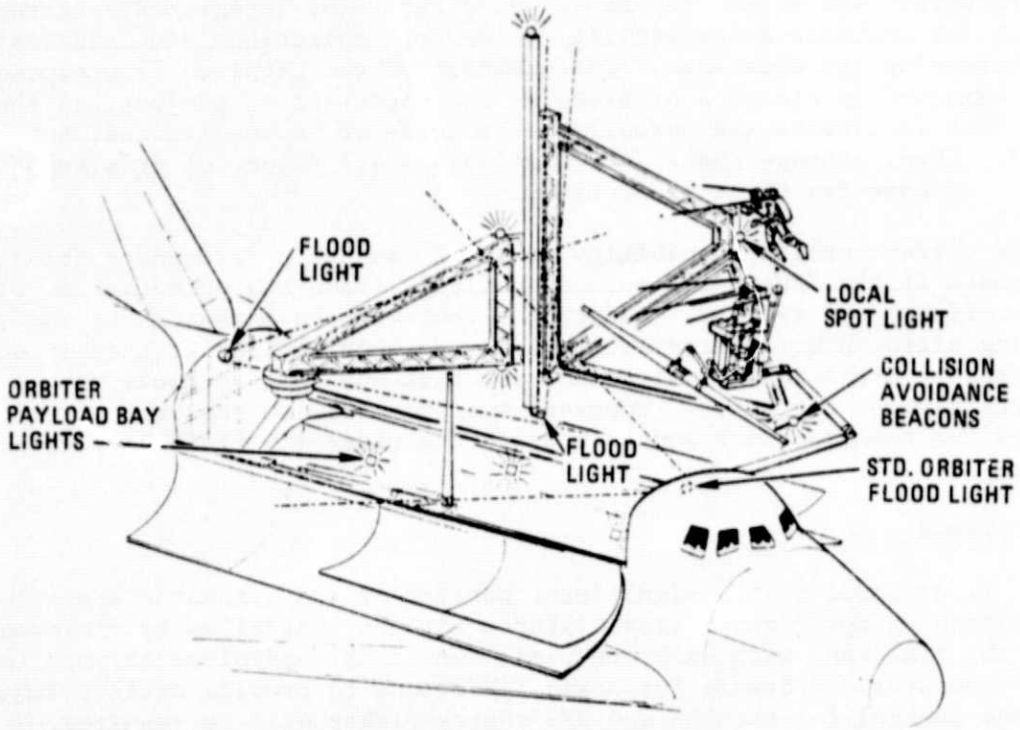

Figure 2.6-1. Space Construction Lighting Concept

Also, maximum use should be made of localized, portable lighting provided by lamps on the manned maneuvering unit (MMU), the extravehicular mobility unit (space suit), portable (battery powered) lamps, the remote manipulator system (RMS), and the cherry picker.

On the sunlit side of orbit the TV systems, which are provided on the orbiter and construction fixtures for remote viewing of construction operations, may need special automatic protection from direct view of sunlight by means of a combination of shades, sensors, and filter or iris controls. Space construction probably will require a large number of TV cameras with a variety of viewing directions. Manual monitoring of all such cameras could place an unacceptable workload on the crew.

2.7 HEAT REJECTION

During the construction of large structures in space, the free interaction of the orbiter with its environment will be modified. In particular, elements of the structure may either block incoming thermal radiation or intercept and reradiate it toward the orbiter. In the first case, heat loads on the orbiter would be decreased. Of greater concern is the second case, in which reradiated (and reflected) radiation may overburden the capabilities of the orbiter radiators.

There are two basic flight system projects under consideration, the SPS test article and the communications platform. However, different orientations and stages of construction multiply the number of cases so that a complete survey of all of them is not practical at this time. In order to achieve an understanding of the magnitude of the problem, several cases (which are believed to be representative of worst-case conditions) have been analyzed. Because the SPS test article presents a large area occupied by an opaque solar blanket, it is believed to be the structure more likely to overheat the orbiter radiators. Two basic construction patterns have been considered in which the array is oriented vertically (see Figure 2.7-1) and transversely (Figure 2.7-2) with respect to the orbiter. In each case, the linear structure is translated past the orbiter while the solar array blanket is unrolled and attached, bay by bay. Clearly, the thermal effect of the array on the orbiter will increase progressively as the amount of structure covered by the solar array blanket increases. In order to assess this, two stages were considered for each orientation—an early stage where one 20×41.6-m bay has been covered, and the final stage where all five bays have been covered.

The relevant thermal properties of the solar array and the orbiter radiators were taken from a recent Rockwell study. The radiation incident on the solar blanket was estimated from the curves provided in a NASA study, *Simplified Thermal Estimation Techniques for Large Space Structures*, NASA CR 145253, October 1977. During construction the orbiter and structure are in a free-drift mode and thus may take any orientation. A most unfavorable one was assumed for the present analysis. The array was assumed to receive solar radiation at normal incidence and earth radiation (emission and albedo) from the side. Table 2.7-1 summarizes the properties and conditions for the numerical calculations, and the appendix presents the results of the thermal analysis.

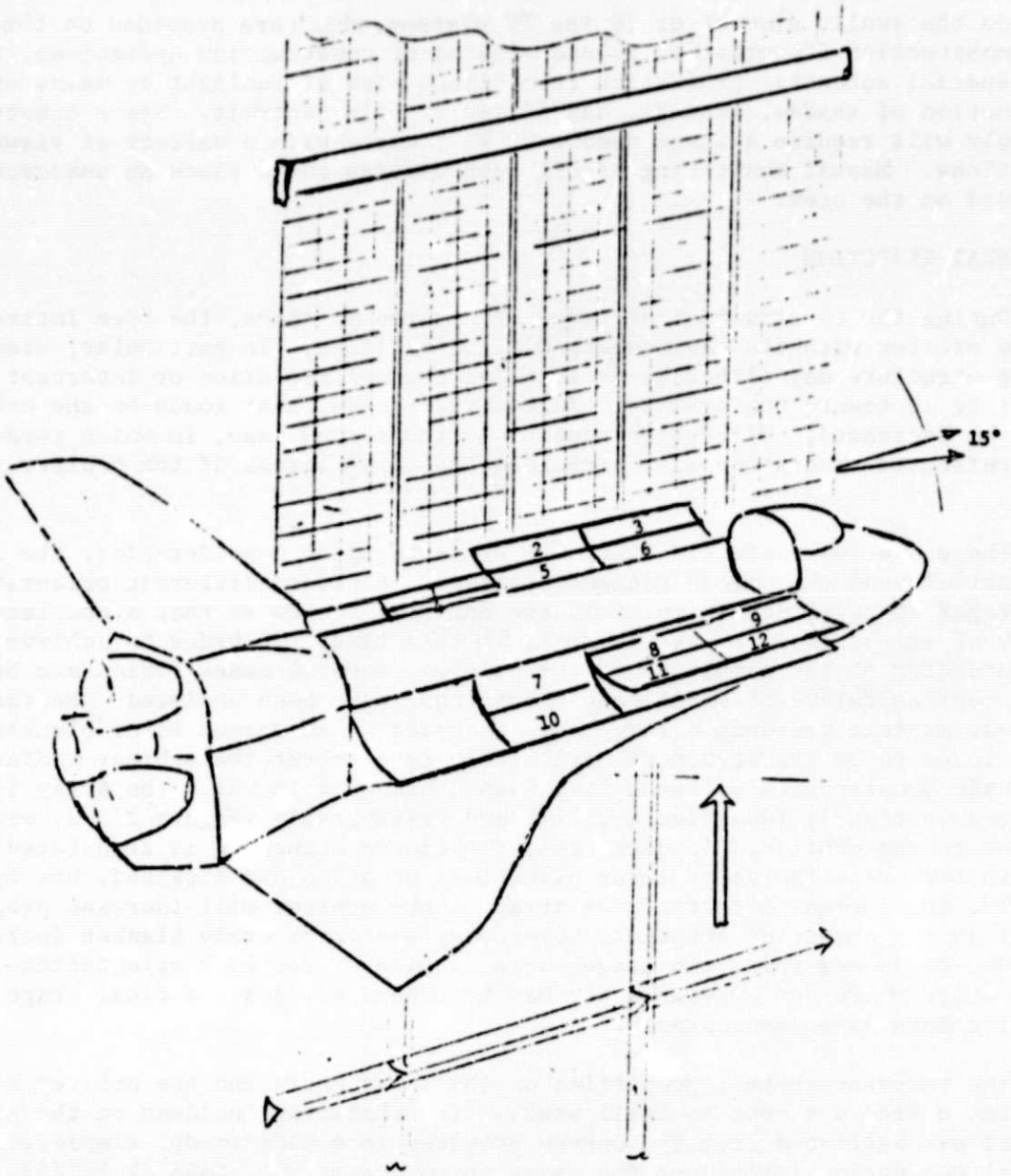

Figure 2.7-1. SPS Test Article Z-Axis Construction Orientation

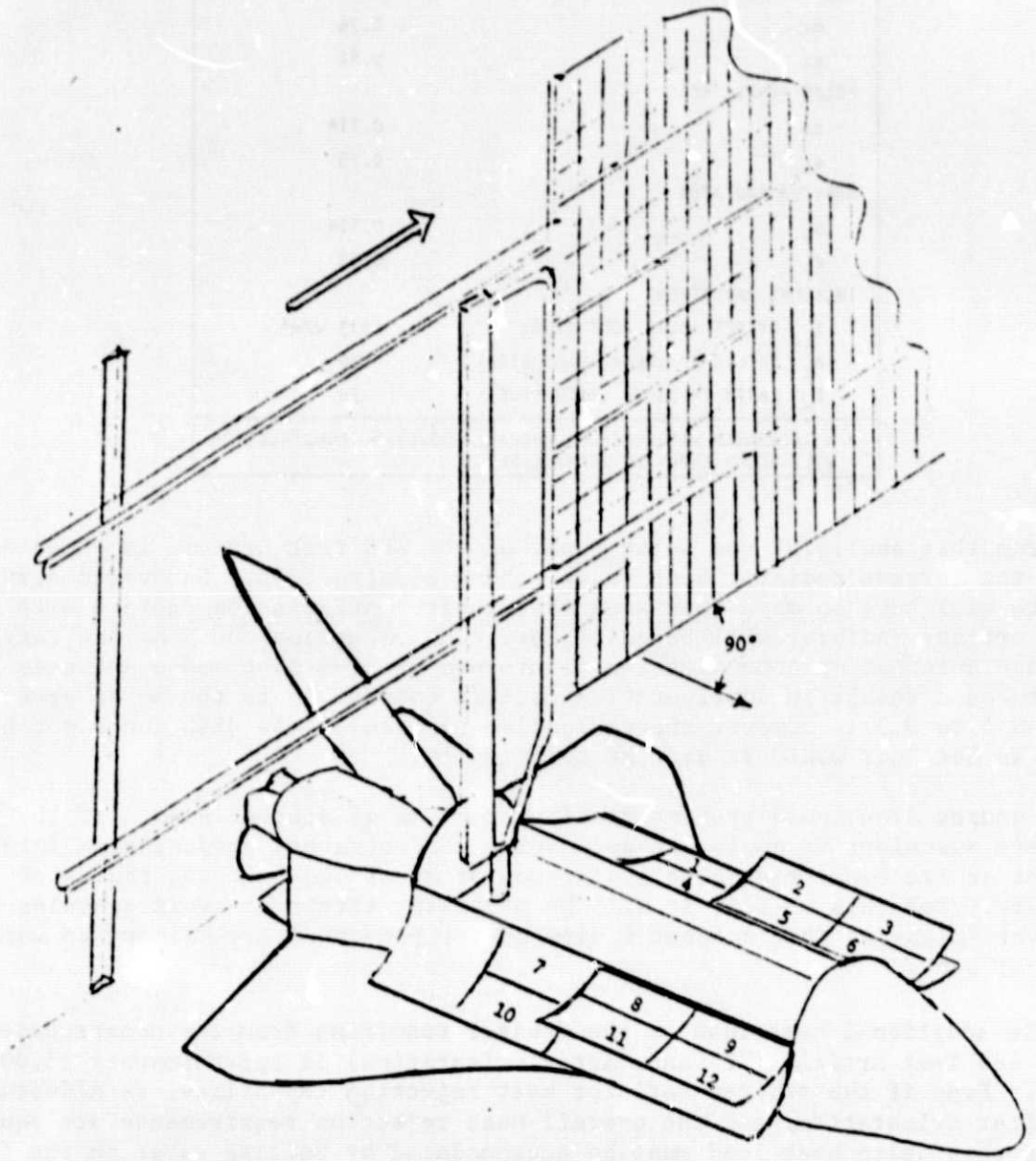

Figure 2.7-2. SPS Test Article Y-Axis Construction Orientation

Table 2.7-1. Thermal Properties and Environmental Factors

	ASSUMED VALUE
SOLAR PANEL, FRONT	
α_1	0.76
ϵ_1	0.82
SOLAR PANEL, REAR	
α_2	0.11*
ϵ_2	0.75
ORBITER RADIATOR	
α_r	0.11*
ϵ_r	0.75
INCIDENT RADIATION	
I_{sc} DIRECT SOLAR (ONE SIDE)	1353 W/m^2
A_l REFLECTED SOLAR (EACH SIDE)	130
E_m EARTH EMISSION (EACH SIDE)	70

* α INCREASES WITH SPACE EXPOSURE. HOWEVER, CONSTRUCTION WILL OCCUR EARLY IN ARRAY LIFE.

From this analysis, the solar panel of the SPS test article is expected to create the largest radiator heat loads during construction. Uncovered structural elements will have so much open area that their configuration factors with respect to the orbiter radiator will be quite low. One exception could be the large microwave antennas on communication platforms. A 20-m dish above and near the orbiter could result in configuration factors comparable to the solar array (e.g., 0.1 to 0.3). However the reflective surface of the dish would not be nearly as hot, nor would it emit as efficiently.

A nearby dish could present heating problems of another kind. If the surface were specular, it could act as a solar concentrator, producing an intense hot spot in its focal region at a distance of about one-half the radius of curvature. For this reason, it will be necessary either to avoid specular surfaces, or to ensure that neither equipment nor personnel are allowed to enter the focal zone.

The additional heat load on the orbiter resulting from the construction of the SPS Test Article ("Y" axis array orientation) is approximately 15,000 BTU/hr. Even if the orbiter radiator heat rejection capability, as affected by orbiter orientation, and the overall heat rejection requirements are equal so that this delta heat load must be accommodated by boiling water in the flash evaporator, no problem is created. 15,000 BTU/hr is equivalent to approximately 15 lbs/hr of water. The water boiling capability of the flash evaporator is 31 lbs/hr and approximately 16 lbs/hr of water is being generated by the fuel cells.

3.0 STRUCTURAL PROVISIONS

Packaging of cargo to fly on the Shuttle must be given careful consideration so that neither the material being carried nor the orbiter will be damaged as a result of the liftoff and landing forces. Location of the cargo in the bay is also of concern to assure proper orbiter control capability during the flight to orbit and return operations.

A cargo cradle concept, which will interface with the orbiter payload support attachment fittings, will minimize the ground operations task of packaging the various construction and project components. The cradle will allow prepackaging of a payload manifest in advance of the installation into the payload bay. The prepackaging operation will consider the c.g. limitations and the on-orbit accessibility requirements.

3.1 LANDING AND LIFTOFF LOADS

The orbiter provides structural support attachment points along the length of the cargo bay as indicated on Figure 3.1-1. Of the potential 172 attach points on the longerons, 118 are normally usable for nondeployable payloads and 102 for deployable payloads. Some potential attach points are unusable because of payload bay door drive linkage, remote manipulator system base and supports, and orbiter system components. There are 117 attach points along the keel. These attach points, longeron and keel, are only available with the use of bridge fittings. The standard longeron bridge fitting is illustrated in Figure 3.1-2, and the keel bridge in Figure 3.1-3.

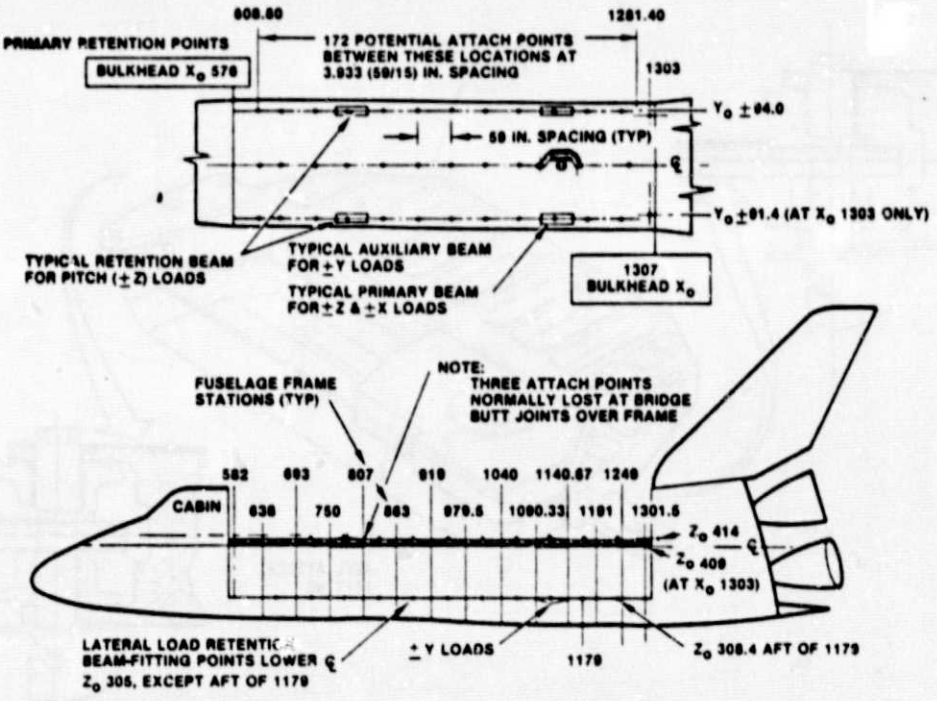

Figure 3.1-1. Standard/Orbiter Payload Attachment Locations

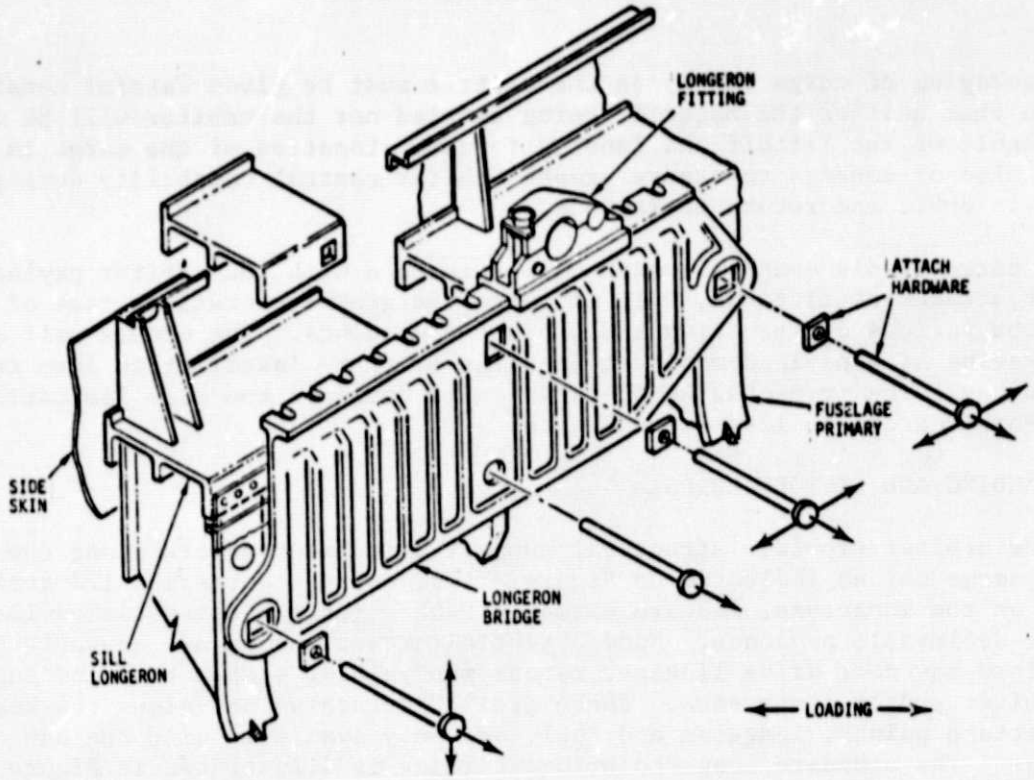

Figure 3.1-2. Longeron Bridge Fitting Installation

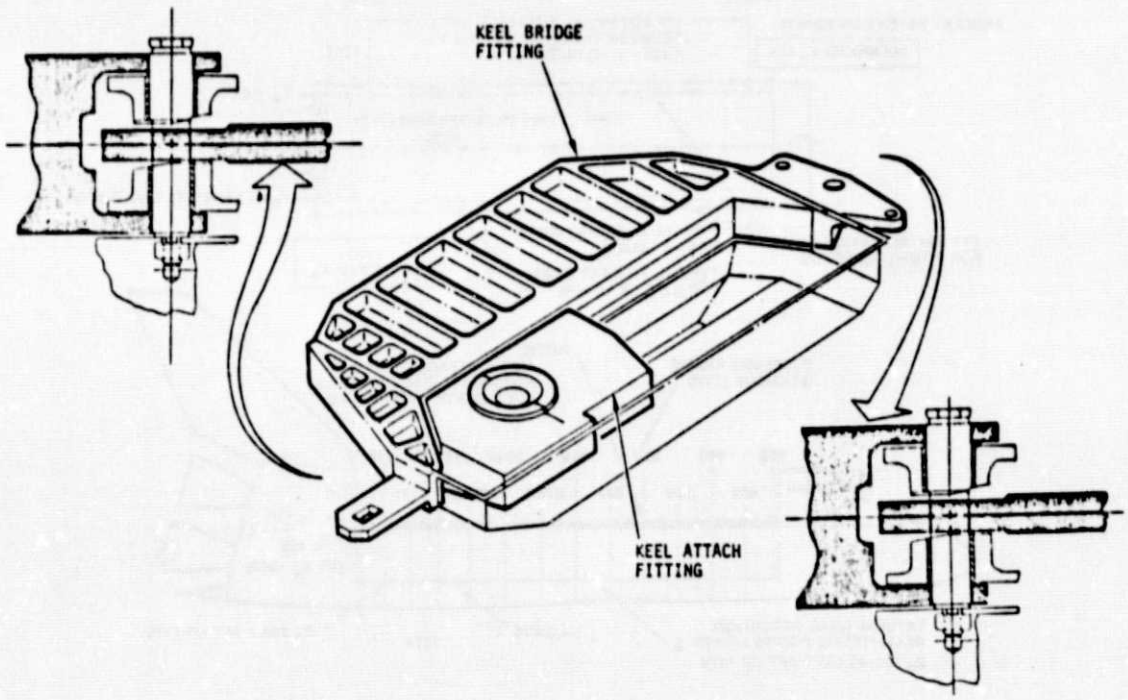

Figure 3.1-3. Keel Bridge and Active Keel Fitting
(Closed Position)

The preliminary limit-load factors and angular accelerations shown in Table 3.1-1 apply to rigid payloads attached directly to the orbiter at any location in the cargo bay. These load factors shall be used for preliminary design of payload primary structure and for determination of preliminary orbiter/payload interface loads. Load factors at specific points within the payload will depend upon payload design characteristics and mounting methods. Payloads that are cantilevered or that have substantial internal flexibility may experience higher load factors than those shown in the table.

Table 3.1-1. Carrier/Payload Design Limit-Load Factors

	LIMIT-LOAD FACTOR*, g			ANGULAR ACCELERATION** RAD/SEC^2			
FLIGHT EVENT	N_X (+ AFT)	N_Y (+ RIGHT)	N_Z (+UP)	θ_X (+ RIGHT WING DN)	θ_Y (+ NOSE UP)	θ_Z (+ NOSE LEFT)	CARRIER / PAYLOAD WEIGHT
ASCENT							
• LIFTOFF	-0.2 -3.2	±1.0	±2.5	±0.1	±0.15	±0.15	
• BOOST MAX, N_X INTEG VEHICLE	-2.9	±0.6	-0.1	±0.2	±0.25	±0.25	UP TO 65K LB
• SRB POST-STAGING	-1.1	±0.12	-0.6				
• BOOST MAX, N_Y ORBITER	-3.17	0.0	-0.6	±0.25	±0.25		
DESCENT							
• TAEM: PITCH MANEUVER	1.01 -0.15	0	2.5	0	0	0	
	0.25	0	2.5	0	-0.11	0	
	0.97	0	-1.0	0	0	0	UP TO 32K LB
	0						
• TAEM: ROLL MANEUVER	0.65	±0.12	1.98	±1.28	0.02	±0.13	
• TAEM: YAW MANEUVER	0.90 0.03	±1.25 ±1.24	1.0 1.0	0 0	0 0	0 ±0.12	
• LANDING	1.8 -2.0	±1.0 ±1.0	4.2 -0.3	±0.25 ±0.25	1.25 0.75	±0.3 ±0.3	

* LIMIT-LOAD FACTOR IS DEFINED AS THE TOTAL EXTERNALLY APPLIED LOAD PER UNIT WEIGHT AT THE c.g. OF THE CARRIER/PAYLOAD AND CARRIES THE SIGN OF THE EXTERNALLY APPLIED LOAD.
** CENTER OF ROTATION IS AT CARRIER/PAYLOAD c.g.

Typical load factors for liftoff and landing are presented. However, during these events, external forces are highly transient and significant elastic response occurs. Payload responses will depend upon payload geometry, stiffness, and mass characteristics. Therefore, until sufficient payload case history is collected, final design values for orbiter payload interface forces and payload design loads must be determined by coupled orbiter payload dynamic analyses for these transient flight events.

To provide for crew safety during emergency landing, the large equipment items, pressure vessels, payload attachments, and supporting structure must withstand the loads associated with the following ultimate load factors, acting separately.

Longitudinal (+ Aft)	Lateral (+ Right)	Vertical (+ Up)
+4.5	+1.5	+4.5
-1.5	-1.5	-2.0

3.2 CENTER OF GRAVITY

All items chargeable to cargo, regardless of location (i.e., within payload bay, below payload bay, in cabin, etc.), shall be included in the calculation to determine the location of the cargo c.g. The cargo c.g.'s shall be constrained within the three limit envelopes defined below:

1. X-Axis—Cargo c.g. shall be calculated using the equations shown in Figure 3.2-1.
2. Y-Axis—Center-of-gravity limits shall be calculated using the equations shown in Figure 3.2-2.
3. Z-Axis—Total cargo c.g. limits shall be calculated using the equations shown in Figure 3.2-3. Center-of-gravity limits for cargo items mounted on the payload bay attachments shall be as shown in Figure 3.2-3. In addition to these cargo Z_O c.g. limits, the Z_O c.g. limits for the summation of all payloads mounted on attachment fittings in the payload bay are defined by curve ABCDEFGHIJ (Figure 3.2-3).

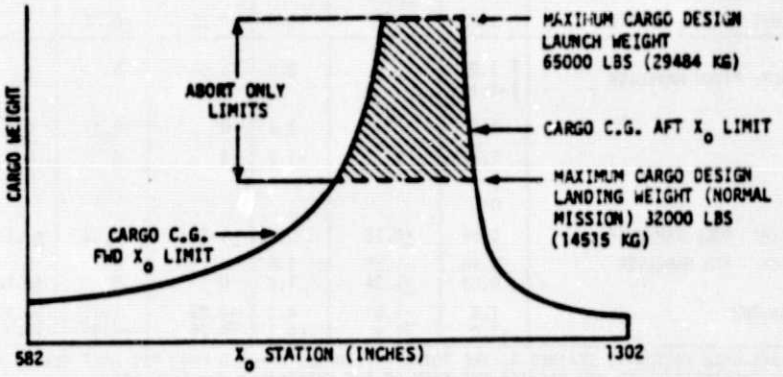

EQUATIONS FOR CALCULATING CARGO X_o (STATION) C.G. LIMITS

$$\text{FWD LIMIT} = \frac{1076.7\ W_c - 3.70 \times 10^6}{W_c}$$

$$\text{AFT LIMIT} = \frac{1108.95\ W_c + 3.4 \times 10^5}{W_c}$$

WHERE W_c = CARGO WEIGHT IN LBS

Figure 3.2-1. Allowable Cargo C.G. Limits (Along X-Axis)

During an abort, if the cargo c.g. is not within the entry and landing design limits, the orbiter (with cargo included) must provide the means to attain an in-limits c.g. location prior to (1) ET separation, for an RTLS abort; or (2) entry and landing, for an on-orbit abort. The orbiter shall similarly be capable of accommodating OMS kit(s) c.g. variations.

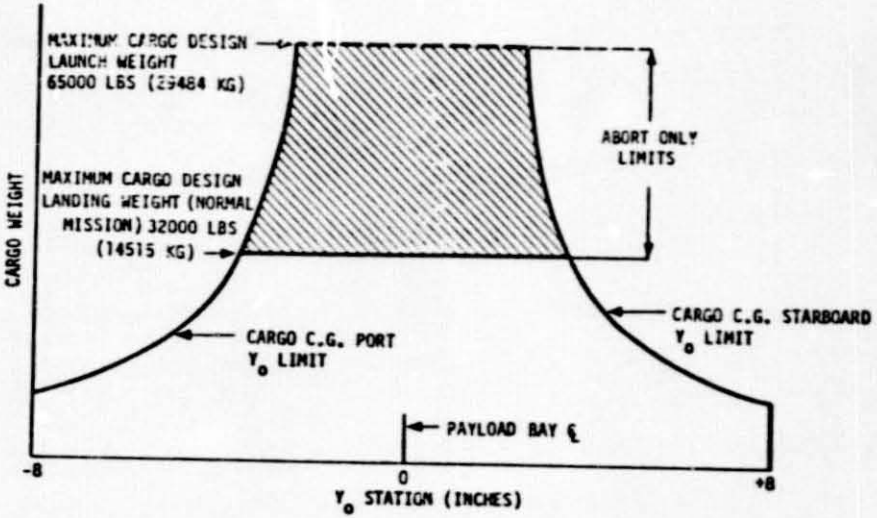

EQUATIONS FOR CALCULATING CARGO Y_o (STATION) C.G. LIMITS

$$\text{LIMIT} = \pm\left[\frac{1.5\,W_c + 6.265\times10^4}{W_c}\right]$$

WHERE W_c = CARGO WT IN LBS

Figure 3.2-2. Allowable Cargo C.G. Limits (Along Y-Axis)

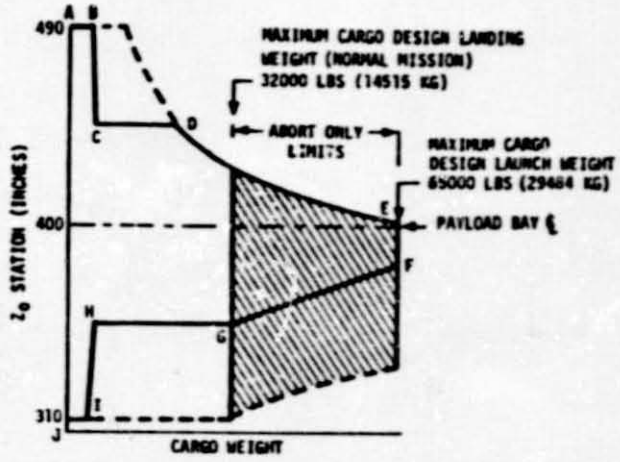

EQUATIONS FOR CALCULATING CARGO Z_o (STATION) C.G. LIMITS

$$\text{UPPER LIMIT} = \frac{384.5\,W_c + 1.331\times10^6}{W_c}$$

$$\text{LOWER LIMIT} = \frac{360\,W_c - 1.566\times10^6}{W_c}$$

WHERE W_c = CARGO WT IN LBS

PARTIAL PAYLOAD Z_o (STATION) C.G. LIMITS FOR SUMMATION OF ALL PAYLOADS MOUNTED ON ATTACHMENT FITTINGS IN PAYLOAD BAY (Z_o C.G. TO REMAIN WITHIN CURVE ABCDEFGHIJ, THE SEGMENTS OF WHICH ARE DEFINED BELOW)

IJAB: SAME AS CARGO C.G. LIMITS ABOVE FOR P/L WT UP TO 4000 LBS

BC: STRAIGHT LINE FROM POINT B (4000 LBS, STA 490) TO POINT C (6000 LBS, STA 445)

CD: STRAIGHT LINE AT STA 445 FROM POINT C (6000 LBS) AND POINT D ON CARGO C.G. LIMITS ABOVE

DEF: SAME AS CARGO C.G. LIMITS ABOVE FROM POINT D (STA 445) TO POINT F (STA 380)

FG: STRAIGHT LINE FROM POINT F(65,000 LBS, STA 380) TO POINT G (32,000 LBS, STA 355)

GH: STRAIGHT LINE AT STA 355 FROM POINT G (32,000) TO POINT H (6000 LBS)

HI: STRAIGHT LINE FROM POINT H(6000 LBS, STA 355) TO POINT I(4000 LBS, STA 310)

Figure 3.2-3. Allowable Cargo C.G. Limits (Along Z-Axis)

4.0 GROUND OPERATIONS

A preliminary investigation of the ground operation for space construction cargos at KSC indicates the advisability of having a facility similar to the Operations and Checkout (O&C) building used by Spacelab. While there will be no functional interfaces between cargo elements, the need for physical integration is expected to be a time-consuming operation. This problem can be minimized by a dedicated "staging" area where the individual items of the cargo can be accumulated, checked out, and packaged into a cargo cradle compatible with the orbiter structural attach provisions. The lack of functional interfaces between the cargo and cargo elements and the minimal functional interfaces between the cargo and the orbiter eliminate the need for any orbiter functional simulator. Thus, the ground support equipment need only include a simple physical simulation of the orbiter cargo bay and all necessary slings, strong backs, cranes, etc., to handle the cargo elements. All preparation of the cargo will be performed "off line" and thus not impact the standard ground turnaround time for the orbiter. The facility will include the capability to install the various cargo elements into the standard cargo cradle for transportation to the orbiter for transfer to the payload bay in the horizontal position at the Orbiter Processing Facility (OPF).

APPENDIX

CALCULATIONS OF THERMAL EFFECTS OF SOLAR ARRAYS ON ORBITER RADIATORS

A preliminary analysis was performed of the heat-rejection capability of the orbiter during a worst-case orientation for constructing the solar array assembly of the SPS test article project. For this case, the solar array surfaces receive direct solar radiation on one side and reflected solar and earth emission radiation on both sides. The key thermal properties and environmental factors are listed in Table A-1. For simplicity, it will be assumed that thermal gradients through the panel are negligible and that the temperature is always steady state. During normal panel operation, a fraction of the absorbed energy is removed in the form of electrical power. However, during construction, all absorbed energy must be reradiated and the panel will run hotter as a result. An energy balance yields the following expression for panel temperature:*

$$T_p = 4\sqrt{\frac{(I_{sc}+A_\ell)\ \alpha_1+A_\ell\alpha_2+E_m\ (\varepsilon_1+\varepsilon_2)}{\sigma\ (\varepsilon_1+\varepsilon_2)}} \qquad \text{(A-1)}$$

For the values in Table A-1, the panel temperature reaches 344°K (71°C).

Table A-1. Thermal Properties and Environmental Factors

	ASSUMED VALUE
SOLAR PANEL, FRONT	
α_1	0.76
ε_1	0.82
SOLAR PANEL, REAR	
α_2	0.11*
ε_2	0.75
ORBITER RADIATOR	
α_r	0.11*
ε_r	0.75
INCIDENT RADIATION	
I_{sc} DIRECT SOLAR (ONE SIDE)	1353 W/m²
A_ℓ REFLECTED SOLAR (EACH SIDE)	130
E_m EARTH EMISSION (EACH SIDE)	70

* α INCREASES WITH SPACE EXPOSURE. HOWEVER, CONSTRUCTION WILL OCCUR EARLY IN ARRAY LIFE.

*Mathematical nomenclature is defined in Table A-4 at the end of this appendix.

The opened radiator panels of the orbiter lie roughly in a plane perpendicular to the solar panel under construction (see Figures A-1 and A-2. For the purposes of this study, the radiator has been subdivided into 12 equal rectangular areas, assumed to be plane and exactly perpendicular to the solar panel. It has been further assumed that the individual areas are small enough to be treated as differentials with respect to the entire solar panel. The idealized relationship is shown in Figure A-3.

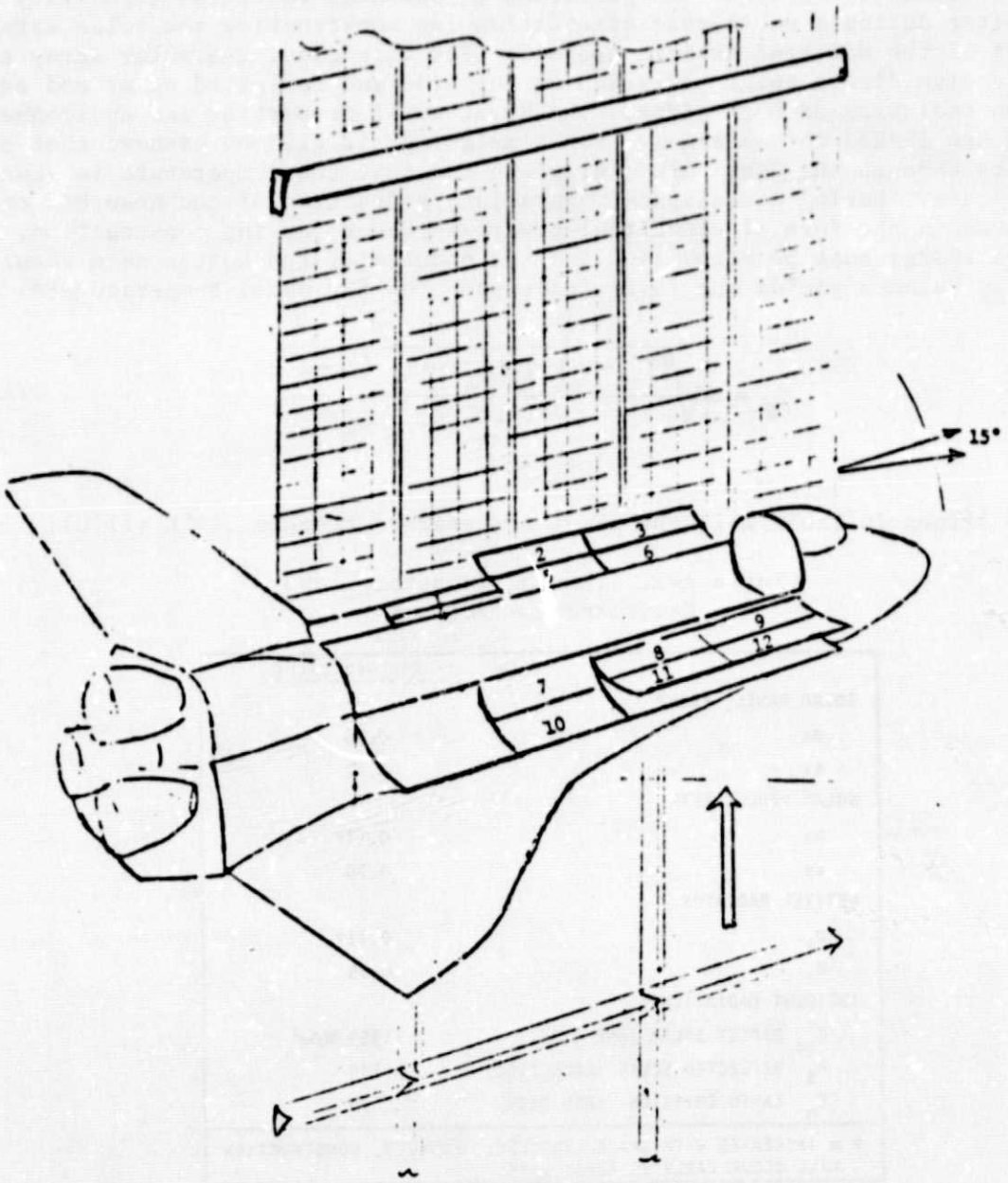

Figure A-1. SPS Test Article Z-Axis Construction Orientation

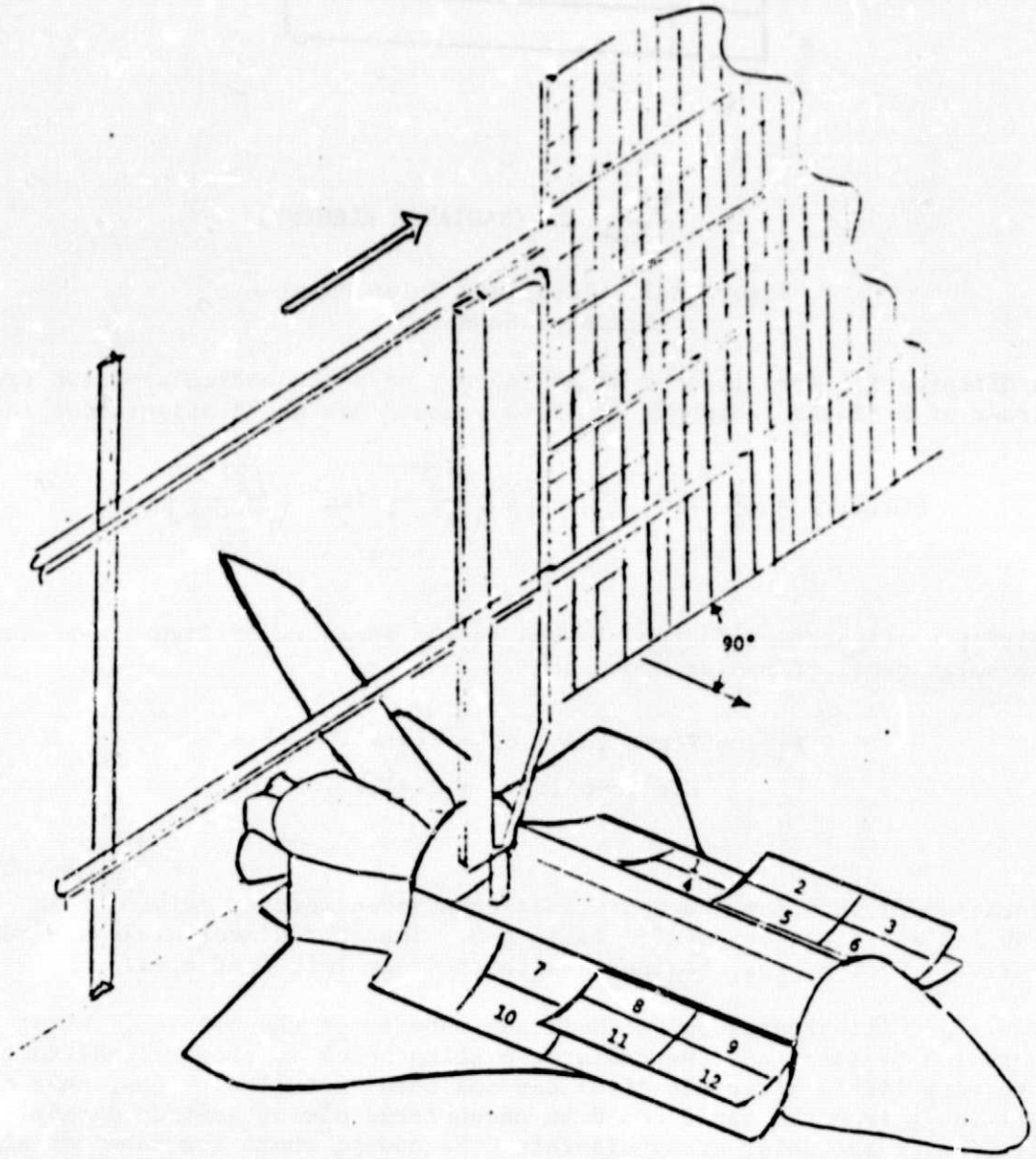

Figure A-2. SPS Test Article
Y-Axis Construction Orientation

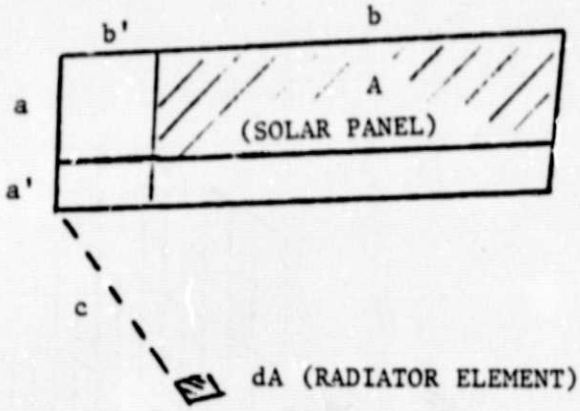

Figure A-3. Idealized Solar Panel—
Radiator Geometry

A differential area located at distance γ on a perpendicular drawn from the corner of a finite rectangle of sides α and β has the configuration factor

$$F(\alpha,\beta,\gamma) = \frac{1}{2\pi}\left[\mathrm{Tan}^{-1}\left(\frac{\beta}{\gamma}\right) - \left(\frac{\gamma}{\beta}\right)\sqrt{\frac{\beta^2}{\alpha^2+\gamma^2}}\,\mathrm{Tan}^{-1}\sqrt{\frac{\beta^2}{\alpha^2+\gamma^2}}\right] \qquad \text{(A-2)}$$

By applying configuration factor algebra to the geometry of Figure A-3, values for the solar panel offset as shown are

$$F_{AdA} = F(a+a^1,b+b^1,c) - F(a+a^1,b^1,c) - F(a^1,b+b^1,c) + F(a^1,b^1,c) \qquad \text{(A-3)}$$

Configuration factors for the four cases considered were calculated from Equation A-3 and are tabulated in Table A-2. The 12 radiator areas are numbered consecutively, row by row, beginning with the rear left-hand area.

Table A-2 illustrates two significant aspects of the problem. First, the configuration factors, and the radiator heating which is proportional to them, increase very little after the first bay has been installed. Thus, near maximum heat loads from the panel could be encountered almost anytime during the installation of the solar array blankets. Secondly, there are substantial differences in heat load, depending on the construction pattern. Transverse construction is clearly less demanding from the thermal point of view.

Radiator heat loads due to the presence of the solar panel under construction arise both from thermal emission and from diffuse reflection of the incident solar radiation. The emission load on a given element of area is

$$\frac{d\dot{Q}_e}{dA_i} = (\varepsilon_i \varepsilon_r \sigma T_p^4)\, F_i \qquad \text{(A-4)}$$

Table A-2. Solar Panel—Radiator Area Configuration Factors

RADIATOR AREA NO.	VERTICAL CONSTRUCTION		TRANSVERSE CONSTRUCTION	
	ONE BAY	FIVE BAYS	ONE BAY	FIVE BAYS
1	.393	.399	.090	.091
2	.308	.315	.202	.205
3	.178	.187	.170	.175
4	.349	.357	.077	.078
5	.285	.294	.177	.180
6	.180	.191	.153	.157
7	.219	.238	.020	.021
8	.186	.206	.072	.073
9	.144	.165	.081	.084
10	.196	.218	.015	.015
11	.168	.190	.057	.058
12	.137	.160	.069	.071

If it is assumed that all reflected solar radiation is isotropic, the additional thermal load is

$$\frac{d\dot{Q}_r}{dA_i} = \left(I_{sc} \frac{(1-\alpha_r)}{\pi} \varepsilon_r \right) F_i dA_i \qquad \text{(A-5)}$$

The sum of the two loads has been integrated over the entire orbiter radiator. The results are given in Table A-3.

Table A-3. Heat Loads on Orbiter Radiators During SPS Test Article Construction

	THERMAL LOAD FROM ARRAY (WATTS)	
	ONE BAY COMPLETED	FIVE BAYS COMPLETED
VERTICAL ("Z" AXIS) ARRAY ORIENTATION:		
ARRAY EMISSION	8600	9100
REFLECTED SOLAR	1400	1500
TOTAL	10000	10600
TRANSVERSE ("Y" AXIS) ARRAY ORIENTATION:		
ARRAY EMISSION	3700	3800
REFLECTED SOLAR	600	600
TOTAL	4300	4400

As may be seen, the thermal loads are substantial, particularly for the vertical construction pattern. For comparison purposes, the unobstructed heat-rejection capability for the orbiter radiator system varies from 5900 watts (20,000 Btu/hr) under unfavorable orientation to 29,300 watts (100,000 Btu/hr) when viewing deep space.

The mathematical nomenclature is defined in Table A-4.

Table A-4. Mathematical Nomenclature

Symbol	Explanation
a, a'	See Figure A-3
A	Area
A_ℓ	Reflected solar radiation
b, b', c	See Figure A-3
F	Configuration factor
E_m	Earth emission radiation
I_{sc}	Solar constant
$\dot{Q}$	Energy flow rate
T	Absolute temperature
Greek Letters	
α	Solar absorptivity
α β δ	Rectangular coordinates
ε	Thermal emissivity
θ	Angle between panel and orbiter operations
σ	Stefan-Boltzmann constant
Subscripts	
1	Front surface
2	Near surface
e	Emitted
i	Area element i
p	Solar panel